

# Chirality-Dependent Vapor-Phase Epitaxial Growth and Termination of Single-Wall Carbon Nanotubes

Bilu Liu,<sup>†,§</sup> Jia Liu,<sup>†,§</sup> Xiaomin Tu,<sup>‡</sup> Jialu Zhang,<sup>†</sup> Ming Zheng,<sup>\*,‡</sup> and Chongwu Zhou<sup>\*,†</sup>

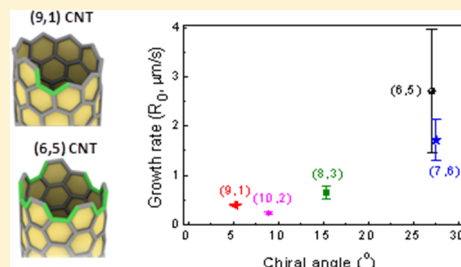
<sup>†</sup>Department of Electrical Engineering and Department of Chemistry, University of Southern California, Los Angeles, California 90089, United States

<sup>‡</sup>National Institute of Standards and Technology, Gaithersburg, Maryland 20899, United States

## S Supporting Information

**ABSTRACT:** Structurally uniform and chirality-pure single-wall carbon nanotubes are highly desired for both fundamental study and many of their technological applications, such as electronics, optoelectronics, and biomedical imaging. Considerable efforts have been invested in the synthesis of nanotubes with defined chiralities by tuning the growth recipes but the approach has only limited success. Recently, we have shown that chirality-pure short nanotubes can be used as seeds for vapor-phase epitaxial cloning growth, opening up a new route toward chirality-controlled carbon nanotube synthesis. Nevertheless, the yield of vapor-phase epitaxial growth is rather limited at the present stage, due in large part to the lack of mechanistic understanding of the process. Here we report chirality-dependent growth kinetics and termination mechanism for the vapor-phase epitaxial growth of seven single-chirality nanotubes of (9, 1), (6, 5), (8, 3), (7, 6), (10, 2), (6, 6), and (7, 7), covering near zigzag, medium chiral angle, and near armchair semiconductors, as well as armchair metallic nanotubes. Our results reveal that the growth rates of nanotubes increase with their chiral angles while the active lifetimes of the growth hold opposite trend. Consequently, the chirality distribution of a nanotube ensemble is jointly determined by both growth rates and lifetimes. These results correlate nanotube structures and properties with their growth behaviors and deepen our understanding of chirality-controlled growth of nanotubes.

**KEYWORDS:** Carbon nanotube, chirality, vapor-phase epitaxy, growth rate, lifetime, termination mechanism



Single-wall carbon nanotubes (SWCNTs) can be conceptually considered as roll up cylinders from graphene sheets.<sup>1</sup> The structure of a SWCNT is uniquely determined by a pair of integers,  $(n, m)$ , named chiral indices, or equivalently, diameter ( $d$ ) and chiral angle ( $\theta$ ). The electronic and optical characteristics of SWCNTs rely on their chiralities,<sup>2,3</sup> and chirality-controlled preparation is crucial for both basic research and many practical applications of SWCNTs in electronics,<sup>4</sup> optoelectronics,<sup>5</sup> and biomedical imaging.<sup>6</sup> For example, Dai et al. have recently reported that chirality-enriched (6, 5) SWCNTs are much brighter than as-synthesized nanotube mixtures in photoluminescence on a premass basis in the IR region, which results a much lower required injected dose for clear tumor imaging.<sup>7</sup> Direct controlled synthesis<sup>8–18</sup> has demonstrated a certain degree of success to control the structures and properties of SWCNTs but is still far away from the goal of single-chirality growth. In addition, the growth mechanism, especially chirality-dependent growth behavior of nanotubes, has not been well understood yet, which brings difficulty toward chirality-controlled synthesis of nanotubes. From a synthetic point of view, the final product distribution, that is, the population of each  $(n, m)$  SWCNT, can be expressed as

$$P(n, m) \propto \int_0^t N(n, m, t, \dots) \times R(n, m, t, \dots) dt \quad (1)$$

Here,  $P$  is the population,  $N$  is the nucleation density,  $R$  is the growth rate, and  $t$  is the growth time for specific  $(n, m)$  SWCNT. This formula shows certain similarity to the one recently proposed by Yakobson et al. on the mass population of SWCNTs.<sup>19</sup> Therefore, the population of each SWCNT is jointly determined by  $N$  and  $R$ , corresponding to the nanotube nucleation and growth steps, respectively. It is speculated that both steps may be dependent on the chirality of nanotubes, and are influenced by a vast amount of experimental parameters, for example, catalysts, catalyst supports, and their pretreatments,<sup>8,9,11–13,15,20</sup> growth time,<sup>21</sup> temperature,<sup>8,15,22</sup> carbon precursors, and their feeding rates,<sup>10</sup> making chirality-controlled SWCNT synthesis an intractable task.

Previous theoretical simulations have investigated the nanotube nucleation processes and revealed chirality-dependent nucleation possibilities (or nucleation density  $N$ ) based on thermodynamic considerations.<sup>23,24</sup> However, experimental observation of chirality-dependent nanotube nucleation is extremely challenging owing to their very fast nucleation dynamics<sup>25</sup> and very small scale,<sup>26</sup> which require characterization methods to have ultrafast response time and ultrahigh spatial resolution. Following nucleation is the nanotube growth

Received: June 20, 2013

Revised: August 8, 2013

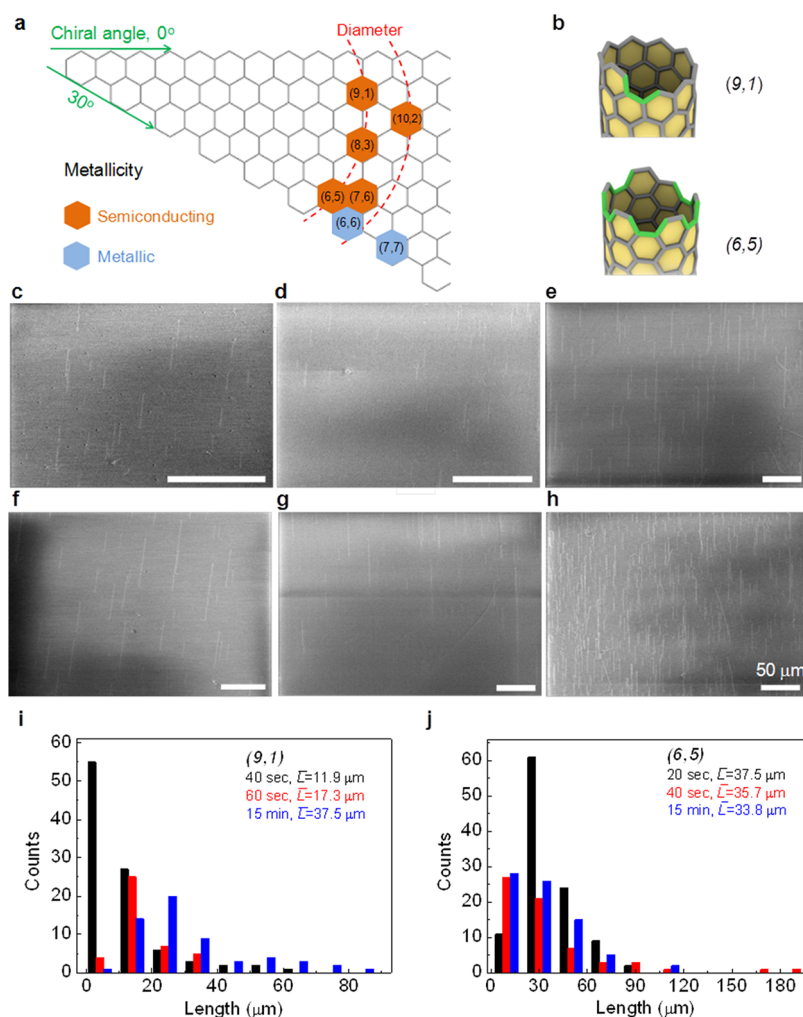


**Figure 1.** Chirality-dependent growth and length distribution of semiconducting (9, 1) and (6, 5) SWCNTs. (a) Chirality map and chiral angle, diameter, and metallicity information of seven nanotubes we studied. (b) Edge structure information of (9, 1) and (6, 5) nanotubes. (c–e) SEM images of VPE-grown (9, 1) SWCNTs with growth time of 40 s, 60 s, and 15 min, respectively. (f–h) SEM images of VPE-grown (6, 5) SWCNTs with growth time of 20 s, 40 s, and 15 min, respectively. (i,j) Length distribution of nanotubes from (c–e) and (f–h), respectively. Scale bars are 50  $\mu\text{m}$  for all images.

kinetics (elongation), which is characterized by the chirality-dependent nanotube growth rate ( $R$ ) and lifetime ( $\tau$ ). Chirality-dependent growth rate has only very recently been discussed in metal-catalyzed chemical vapor deposition (CVD) process,<sup>27,28</sup> while the chirality-dependent growth lifetime ( $\tau$ ) of nanotubes, as far as we know, has not been studied. We note that in nearly all nanotube synthetic methods including CVD, arc discharge, and laser ablating, neither nucleation nor growth step can be fixed or isolated, making chirality-controlled growth an elusive goal. Recently, we have developed a vapor phase epitaxial (VPE) based cloning strategy that uses DNA-separated chirality-pure nanotube seeds for chirality-controlled synthesis of SWCNTs.<sup>29</sup> The uniqueness of such process is that the single-chirality nanotube seeds, which initiate succeeding nanotube growth, are pre-existing already. Thanks to this advantage, the nanotube nucleation step, which has been demonstrated to be an intractable process to control,<sup>23,24</sup> is circumvented. Therefore, the VPE process serves as a valuable platform to unambiguously distinguish nucleation from growth processes and to focus solely on chirality-dependent growth kinetics of SWCNTs. Inspired by this deliberation, in this Letter we have systematically studied a total of seven single-

chirality SWCNTs for VPE cloning growth to investigate the different growth behaviors of these SWCNTs and correlate to their chiralities. Noticeably, the SWCNTs we chose contain both metallic and semiconducting ones, which span a large chiral angle range but with similar diameters, thus singling out the impact of chiral angles on the growth rates and lifetimes of SWCNTs.

The VPE-based cloning process follows our previous report<sup>29</sup> with some improvements (see details in Supporting Information). Previous studies have demonstrated that  $\text{C}_2\text{H}_4$  is a highly effective carbon source for the growth of vertically aligned SWCNT forests<sup>30</sup> and the addition of small amount of  $\text{C}_2\text{H}_4$  into  $\text{CH}_4$  CVD system significantly improves the yield of SWCNTs.<sup>13,31</sup> A small amount (optimized at 10 sccm) of  $\text{C}_2\text{H}_4$  was added into VPE process and the SEM characterization showed the yield of SWCNTs improved significantly with optimal amount of  $\text{C}_2\text{H}_4$  addition (Supporting Information Figures S1 and S2). This yield improvement paves the way for the study of chirality-dependent growth and termination of large amount of SWCNTs.

Figure 1a shows the chirality map of seven kinds of nanotubes we studied in this work. The three important

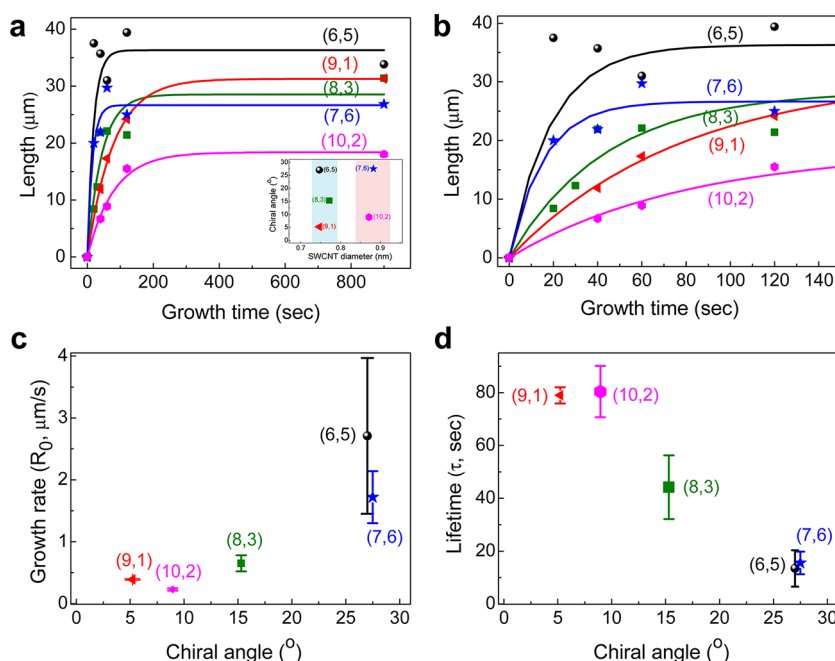


**Figure 2.** Length evolution profiles and chirality-dependent growth rate ( $\bar{R}_0$ ) and lifetime ( $\tau$ ) of semiconducting SWCNTs. (a) Length evolution profiles and fitted curves based on eq 3 for (6, 5), (8, 3), (9, 1), (7, 6), and (10, 2) SWCNTs with growth times of 20 s, 40 s, 60 s, 2 min, and 15 min. Inset, chiral angle versus diameter for the above five semiconducting SWCNTs, showing that they belong to two subgroups with similar diameters in each one as highlighted by different colors. (b) Zoom-in plot of panel a shows the initial growth period. (c,d) Chiral-angle-dependent growth rate ( $\bar{R}_0$ ) and lifetime ( $\tau$ ) of the above five kinds of semiconducting SWCNTs. The vertical error bars in c and d correspond to the errors of parameters extracted based on eq 3.

structural and property parameters of SWCNTs, that is, chiral angle, diameter, and metallicity, are highlighted. As an illustration, Figure 1b compares the edge structures of (9, 1) and (6, 5) SWCNTs, where the differences in their edge-atom-configurations can be clearly discerned. One important question here is how the edge structures of nanotubes influence their growth behaviors.

To obtain information on the growth kinetics of SWCNTs, we performed systematical experiments at different growth times ranging from tens of seconds to 15 min. Figure 1c–e presents SEM images of (9, 1) SWCNTs with growth duration of 40 s, 60 s, and 15 min, respectively. The average nanotube length ( $\bar{L}$ ) for each duration was measured and presented in Figure 1i, which demonstrates that the length of (9, 1) nanotubes keep growing during this period of time. As a comparison, Figure 1f–h shows the SEM images of (6, 5) SWCNTs with growth time of 20 s, 40 s, and 15 min, with the length distribution histogram shown in Figure 1j. In sharp contrast to (9, 1) nanotubes, we found that the (6, 5) nanotubes have nearly the same average lengths with different growth periods, suggesting the active growth lifetime is very short. Note that both (9, 1) and (6, 5) nanotubes are the semiconducting type with identical diameters but distinct chiral angles. Specifically, (6, 5) is a near armchair SWCNT with a chiral angle of 27.0°, while (9, 1) represents a near zigzag SWCNT with a chiral angle of only 5.2°. This result clearly demonstrates the influence of chiral angles on the growth of SWCNTs.

To get in depth and comprehensive information on the growth kinetics, we systematically studied the growth of five types of semiconducting SWCNTs under various growth times, that is, 20, 30, 40, 60, 120, and 900 s (Supporting Information Figure S3, S4, S5, S6, and S7). Colored dots in Figure 2a show

the length evolutions of these five nanotubes. It is evident that these nanotubes possess distinct growth kinetics, especially during the initial growth period, as shown in Figure 2b.

To quantitatively analyze the nanotube growth kinetics and to model the growth process that has a finite period, that is, growth plus termination, we assume the average growth rate ( $\bar{R}_t$ ) of a ( $n, m$ ) SWCNT at time  $t$  follows exponential kinetics

$$\bar{R}_t = \bar{R}_0 \exp\left(-\frac{t}{\tau}\right) \quad (2)$$

Here,  $\bar{R}_0$  and  $\tau$  are the average initial growth rate and lifetime for a SWCNT. Consequently, the average nanotube length ( $\bar{L}_t$ ) at time  $t$  would be

$$\bar{L}_t = \int_0^t \bar{R}_t dt = \bar{R}_0 \tau \left[1 - \exp\left(-\frac{t}{\tau}\right)\right] \quad (3)$$

We used eq 3 to fit the length evolution profiles of the preceding mentioned five SWCNTs (solid curves in Figure 2a) and extracted the two parameters, that is,  $\bar{R}_0$  and  $\tau$  for each nanotube. Here we emphasize that the nanotubes we studied fall into two subgroups with very similar diameters in each subgroup (inset of Figure 2a), thus excluding any effect of nanotube diameter on their growth kinetics.<sup>21,32,33</sup> Since all five of these nanotubes are semiconducting ones, the only noticeable structural parameter difference within each subgroup is the chiral angle. Therefore, the above results suggest a clear chiral angle-dependent growth behavior of SWCNTs.

We further plotted chiral angle versus growth rate and lifetime for these five SWCNTs in Figure 2c,d. As can be clearly discerned from Figure 2c, nanotube growth rate increases with increasing its chiral angle, a result similar to that of a very recent report on metal catalyst driven CVD grown nanotubes.<sup>28</sup> Here we note that for VPE-cloning process, both ends of the seed



nanotubes may be active for growth, a phenomenon different from metal-catalyzed CVD processes where only catalyst-nanotube joint point is active. Consequently, the actual growth rate of each  $(n, m)$  SWCNT may be overestablished by a factor of 2. Nevertheless, this will not have any influence on the trend of chirality-dependent growth rate of SWCNTs we have concluded. In addition to the chirality-dependent growth rates of nanotubes, more interestingly, we observed an opposite trend for chiral angle dependent lifetimes, that is, the lifetime of a nanotube decreases while increasing its chiral angle (Figure 2d). Specifically, both (9, 1) and (10, 2) nanotubes possess lifetimes of  $\sim 80$  s under our growth condition, which are much longer than (8, 3) nanotube with a lifetime of  $\sim 40$  s and (6, 5) and (7, 6) nanotubes with a lifetime of less than 20 s. Therefore, we emphasize that the final product distribution of a SWCNT ensemble neither solely relies on their growth rates nor their active lifetime as understood previously, but on their product  $\bar{R}_0 \times \tau$ .

We propose that the above chirality-dependent growth rate and lifetime phenomena can be interpreted in the framework of Diels–Alder cycloaddition mechanism.<sup>25,29,34</sup> According to the Diels–Alder chemistry, active carbon species will only be added to the armchair sites (serve as dienophile) on the open edges of SWCNTs during VPE-based cloning process.<sup>29</sup> Note that a particular  $(n, m)$  SWCNT has a total of  $m$  armchair sites (Figure 3a,e), which can simultaneously accept coming carbon

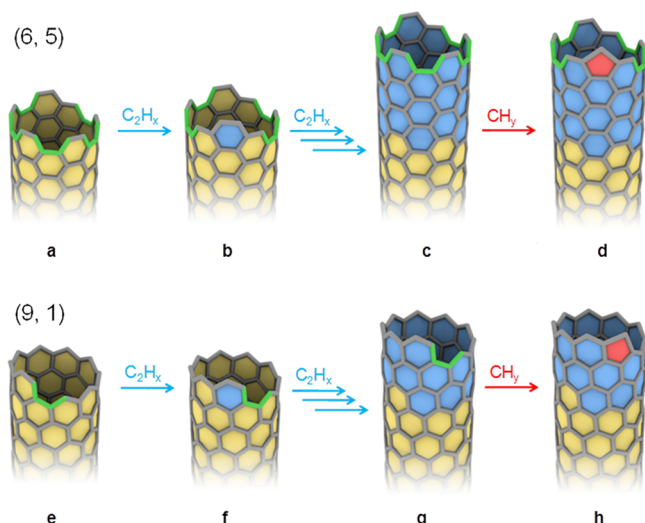


**Figure 3.** Atomic illustration of chirality-dependent SWCNT growth via Diels–Alders cycloaddition processes. (a–c) Cycloaddition of  $C_2H_x$  species to a (6, 5) SWCNT and the formation of six-membered rings, leading to the continuous growth of this nanotube. (d) Addition of  $CH_y$  species leads to the formation of five-membered ring and consequently nanotube growth stops. (e–g) Addition of  $C_2H_x$  species to a (9, 1) SWCNT for its continuous growth. (h) Addition of  $CH_y$  species leads to the growth stops. Multiple arrows from panels b to c and panels f to g represent multiple addition reactions.

species for nanotube growth (Figure 3a–c and Figure 3e–g). Therefore, it is a natural consequence that nanotubes with large  $m$  possess high growth rate. In real nanotube growth process, however, the situation may not be that ideal and we speculate that each adding step has a certain failure possibility. Previous studies on  $CH_4$  pyrolysis show that it follows the sequence of  $CH_4 \rightarrow CH_3 \rightarrow C_2H_6 \rightarrow C_2H_4 \rightarrow C_2H_2 \rightarrow \dots \rightarrow C$  (solid) at temperature of  $\sim 900$  °C.<sup>35,36</sup> Apparently, there exist various

$CH_x$ ,  $C_2H_x$ , and even  $C_3H_x$  species in the CVD environment.<sup>36,37</sup> We note that the addition of  $CH_x$  or  $C_3H_x$  species instead of  $C_2H_x$  will generate five- or seven-membered ring on nanotubes (Figure 3d,h), which in turn may prevent further nanotube growth via Diels–Alder chemistry. On the basis of recent theoretical studies,<sup>25,38</sup> the formation of six-membered ring is more energetically favorable than other kinds of structures especially when the nanotube segment is long. Nevertheless, there is still a very low but certain possibility for five- or seven-membered ring formation, which in turn will terminate nanotube growth. We emphasize that for nanotubes with large  $m$ , the adding events would happen more frequently than those nanotubes with small  $m$ . Consequently, it will take much shorter time for these larger  $m$  nanotubes to form the five- or seven-membered rings than the smaller  $m$  ones from statistical point of view, suggesting a shorter lifetime for nanotubes with larger  $m$ . Note that this does not necessarily mean lifetime is directly proportional to  $1/m$ , as the nanotube diameter may also play a role on its growth.<sup>25,32</sup> Nevertheless, it is safe to conclude, based on the Diels–Alder process illustrated in Figure 3, that SWCNTs with larger  $m$  would have higher growth rates and shorter active lifetimes. This conclusion agrees very well with our experimental observations as for nanotubes with similar diameters, large chiral angle corresponds to large  $m$ . Importantly, we note that a screw dislocation mechanism has been experimentally identified for catalyst-free growth of nanowires in CVD process,<sup>39</sup> which resembles the VPE growth of nanotube via Diels–Alder mechanism, especially for  $(n, 1)$  nanotubes. Consequently, the results in this study connect nanotubes with nanowires and indicate that there might be a general growth mechanism for one-dimensional crystalline nanostructures. The chirality-dependent growth behavior and termination mechanism, however, is not reflected by nanowire growth case. Therefore, the results from this study provide new insight on the controlled growth of one-dimensional nanostructures and materials.

Among all kinds of SWCNTs, armchair  $(n, n)$  nanotubes are of particular interest since they are the only true metallic nanotubes with zero band gap and linear energy dispersion relationships at Dirac point.<sup>40</sup> Our DNA-based separation method is capable of purifying such armchair metallic nanotubes, for example, (6, 6) and (7, 7), with high purity.<sup>41</sup> Here, we chose these two kinds of armchair nanotubes and studied their growth kinetics. Showing in Figure 4a,b are the SEM images of the (6, 6) and (7, 7) SWCNTs with a growth time of 20 s. Surprisingly, we found that both nanotubes have relatively short average length (11.5  $\mu m$  for (6, 6) and 6.4  $\mu m$  for (7, 7)). We further studied the length evolution of these two armchair SWCNTs with growth time of 40 and 60 s (Supporting Information Figure S8). As shown in Figure 4c,d, both nanotubes stop growth within 20 s, indicating a very short lifetime, which is consistent with our experimental observations and Diels–Alder cycloaddition mechanism proposed on large chiral angle SWCNTs. While it is difficult to accurately calculate the growth rate for these two nanotubes since they saturated within the shortest experimental time, we would like to comment on their saturated lengths and compare with their semiconducting counterparts, for example, (6, 6) versus (6, 5). The most noticeable difference is that (6, 6) nanotubes possess much shorter,  $\sim 1/3$ , saturated length as compared with (6, 5) ones, which has never been reported before. One interesting phenomenon we noted is that in real SWCNT samples, armchair ones abnormally do not occupy a large population

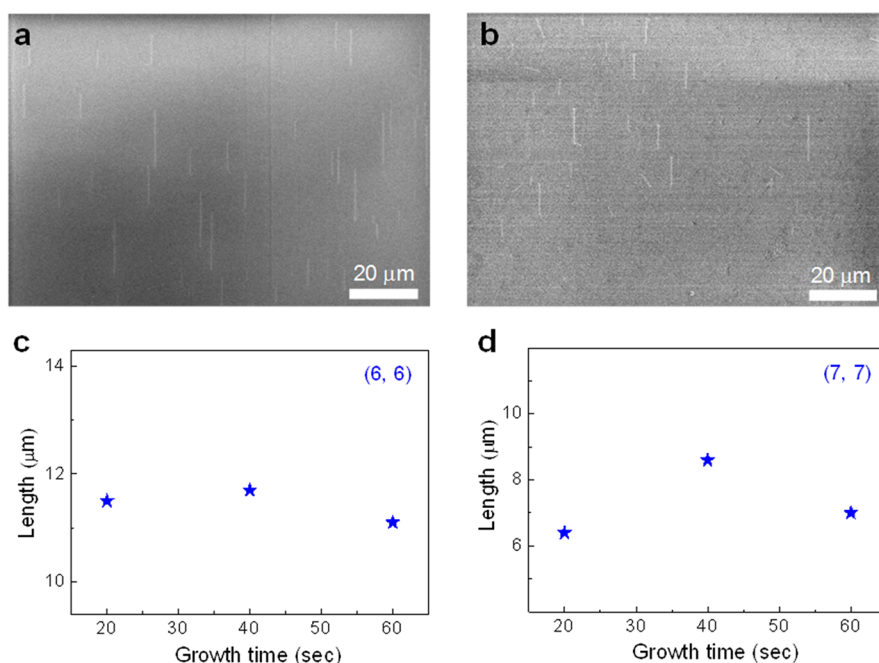


**Figure 4.** Chirality-dependent growth of armchair metallic SWCNTs. (a,b) Representative SEM images of cloned (6, 6) and (7, 7) SWCNTs with a growth time of 20 s. (c,d) Length evolution of (6, 6) and (7, 7) SWCNTs with growth time of 20, 40, and 60 s.

based on the electron diffraction analysis.<sup>42</sup> This result is consistent with our observation here shown that armchair nanotubes possess shorter saturated lengths than other nanotubes, that is, they are less abundant in a nanotube ensemble. We noticed that armchair nanotubes are the only true metallic ones with zero bandgap, thus it is intriguing to study whether the electronic properties of nanotubes have a strong effect on the growth. Further experiments that can well control the growth period into a very short time, for example, a few seconds,<sup>21</sup> combined with theoretical simulations, may help to understand the abnormal behavior of armchair SWCNTs, which may open up a novel window to exploring metallic/semiconducting controlled synthesis. Furthermore, future comparative studies of nonarmchair metallic SWCNTs (e.g., semimetallic SWCNTs<sup>1</sup>), armchair metallic SWCNTs, and semiconducting ones would be important to further determine possible effect of metallicity on the growth of nanotubes, which could not be done at this moment due to lack of chirality-pure nonarmchair metallic SWCNT seeds.

In conclusion, we have isolated nanotube elongation and termination from their nucleation and studied chirality-dependent growth rate and active lifetime of both semiconducting and metallic SWCNTs in a recently established VPE-based cloning platform. Our research reveals distinct growth behaviors among SWCNTs and correlate with their structures within the framework of Diels–Alder chemistry. The abnormal growth behavior of armchair nanotubes suggests a possible correlation between nanotube growth and their electronic characteristics. This work provides direct experimental evidence on the chirality-dependent growth kinetics of single-chirality nanotubes, which can guide further synthetic processes designed toward chirality-pure SWCNT synthesis. Moreover, the similarity of catalyst-free nanotube and nanowire growth indicates that these one-dimensional crystalline nanostructures may follow similar and more general growth mechanism. Our VPE-grown chirality-pure SWCNTs may work as valuable material platform for the applications of nanotubes

in electronics, optoelectronics, and biomedical imaging, where single-chirality nanotubes could greatly improve the device performance. In addition, these chirality-pure SWCNTs may even lead to graphene nanoribbons (GNRs) with well-defined widths and edge structures through the nanotube unzipping process,<sup>43–45</sup> which will significantly push forward GNR research and applications.

## ■ ASSOCIATED CONTENT

### Supporting Information

Experiment details regard single-chirality nanotube separation, nanotube seeds deposition, VPE growth process, and more SEM and Raman characterization. This material is available free of charge via the Internet at <http://pubs.acs.org>.

## ■ AUTHOR INFORMATION

### Corresponding Author

\*E-mail: (C.Z.) [chongwuz@usc.edu](mailto:chongwuz@usc.edu); (M.Z.) [ming.zheng@nist.gov](mailto:ming.zheng@nist.gov).

### Author Contributions

<sup>§</sup>B.L. and J.L. contributed equally to this work.

### Notes

The authors declare no competing financial interest.

## ■ ACKNOWLEDGMENTS

This work was supported by the Office of Naval Research and the Defence Threat Reduction Agency (DTRA). We acknowledge Professor Stephen Cronin of University of Southern California for access to 532 and 633 nm Raman facility, and Professor Boris I. Yakobson of Rice University for helpful discussions.

## ■ REFERENCES

- (1) Jorio, A.; Dresselhaus, G.; Dresselhaus, M. S. *Carbon Nanotubes: Advanced topics in the synthesis, structure, properties and applications*; Springer-Verlag: Berlin Heidelberg, 2008.

- (2) Odom, T. W.; Huang, J. L.; Kim, P.; Lieber, C. M. *Nature* **1998**, *391*, 62–64.
- (3) Wildoer, J. W. G.; Venema, L. C.; Rinzler, A. G.; Smalley, R. E.; Dekker, C. *Nature* **1998**, *391*, 59–62.
- (4) Jin, S. H.; Dunham, S. N.; Song, J.; Xie, X.; Kim, J.-H.; Lu, C. F.; Islam, A.; Du, F.; Kim, J.; Felts, J.; Li, Y.; Xiong, F.; Wahab, M. A.; Menon, M.; Cho, E.; Grosse, K. L.; Lee, D. J.; Chung, H. U.; Pop, E.; Alam, M. A.; King, W. P.; Huang, Y. G.; Rogers, J. A. *Nat. Nanotechnol.* **2013**, *8*, 347–355.
- (5) Avouris, P.; Freitag, M.; Perebeinos, V. *Nat. Photonics* **2008**, *2*, 341–350.
- (6) Welscher, K.; Liu, Z.; Sherlock, S. P.; Robinson, J. T.; Chen, Z.; Daranciang, D.; Dai, H. J. *Nat. Nanotechnol.* **2009**, *4*, 773–780.
- (7) Antaris, A. L.; Robinson, J. T.; Yaghi, O. K.; Hong, G. S.; Diao, S.; Luong, R.; Dai, H. J. *ACS Nano* **2013**, *7*, 3644–3652.
- (8) Chiang, W. H.; Sankaran, R. M. *Nat. Mater.* **2009**, *8*, 882–886.
- (9) Harutyunyan, A. R.; Chen, G. G.; Paronyan, T. M.; Pigios, E. M.; Kuznetsov, O. A.; Hewaparakrama, K.; Kim, S. M.; Zakharov, D.; Stach, E. A.; Sumanasekera, G. U. *Science* **2009**, *326*, 116–120.
- (10) Wang, B.; Poa, C. H. P.; Wei, L.; Li, L. J.; Yang, Y. H.; Chen, Y. *J. Am. Chem. Soc.* **2007**, *129*, 9014–9019.
- (11) He, M.; Chernov, A. I.; Fedotov, P. V.; Obratsova, E. D.; Sainio, J.; Rikkinen, E.; Jiang, H.; Zhu, Z.; Tian, Y.; Kauppinen, E. I.; Niemela, M.; Krauset, A. O. I. *J. Am. Chem. Soc.* **2010**, *132*, 13994–13996.
- (12) Bachilo, S. M.; Balzano, L.; Herrera, J. E.; Pompeo, F.; Resasco, D. E.; Weisman, R. B. *J. Am. Chem. Soc.* **2003**, *125*, 11186–11187.
- (13) Yao, Y. G.; Feng, C. Q.; Zhang, J.; Liu, Z. F. *Nano Lett.* **2009**, *9*, 1673–1677.
- (14) Smalley, R. E.; Li, Y. B.; Moore, V. C.; Price, B. K.; Colorado, R.; Schmidt, H. K.; Hauge, R. H.; Barron, A. R.; Tour, J. M. *J. Am. Chem. Soc.* **2006**, *128*, 15824–15829.
- (15) Liu, B. L.; Ren, W. C.; Li, S. S.; Liu, C.; Cheng, H. M. *Chem. Commun.* **2012**, *48*, 2409–2411.
- (16) Ding, L.; Tselev, A.; Wang, J. Y.; Yuan, D. N.; Chu, H. B.; McNicholas, T. P.; Li, Y.; Liu, J. *Nano Lett.* **2009**, *9*, 800–805.
- (17) Hong, G.; Zhang, B.; Peng, B. H.; Zhang, J.; Choi, W. M.; Choi, J. Y.; Kim, J. M.; Liu, Z. F. *J. Am. Chem. Soc.* **2009**, *131*, 14642–14643.
- (18) Che, Y. C.; Wang, C.; Liu, J.; Liu, B. L.; Lin, X.; Parker, J.; Beasley, C.; Wong, H. S. P.; Zhou, C. W. *ACS Nano* **2012**, *6*, 7454–7462.
- (19) Penev, E. S.; Artyukhov, V. I.; Ding, F.; Yakobson, B. I. *Adv. Mater.* **2012**, *24*, 4956–4976.
- (20) Liu, B. L.; Ren, W. C.; Liu, C.; Sun, C. H.; Gao, L. B.; Li, S. S.; Jiang, C. B.; Cheng, H. M. *ACS Nano* **2009**, *3*, 3421–3430.
- (21) Kato, T.; Hatakeyama, R. *ACS Nano* **2010**, *4*, 7395–7400.
- (22) Miyauchi, Y. H.; Chiashi, S. H.; Murakami, Y.; Hayashida, Y.; Maruyama, S. *Chem. Phys. Lett.* **2004**, *387*, 198–203.
- (23) Yazyev, O. V.; Pasquarello, A. *Phys. Rev. Lett.* **2008**, *100*, 156102.
- (24) Ding, F.; Larsson, P.; Larsson, J. A.; Ahuja, R.; Duan, H. M.; Rosen, A.; Bolton, K. *Nano Lett.* **2008**, *8*, 463–468.
- (25) Li, H. B.; Page, A. J.; Irle, S.; Morokuma, K. *J. Am. Chem. Soc.* **2012**, *134*, 15887–15896.
- (26) Yoshida, H.; Takeda, S.; Uchiyama, T.; Kohno, H.; Homma, Y. *Nano Lett.* **2008**, *8*, 2082–2086.
- (27) Ding, F.; Harutyunyan, A. R.; Yakobson, B. I. *Proc. Natl. Acad. Sci. U.S.A.* **2009**, *106*, 2506–2509.
- (28) Rao, R.; Liptak, D.; Cherukuri, T.; Yakobson, B. I.; Maruyama, B. *Nat. Mater.* **2012**, *11*, 213–216.
- (29) Liu, J.; Wang, C.; Tu, X. M.; Liu, B. L.; Chen, L.; Zheng, M.; Zhou, C. W. *Nat. Comm.* **2012**, *3*, 1199.
- (30) Hata, K.; Futaba, D. N.; Mizuno, K.; Namai, T.; Yumura, M.; Iijima, S. *Science* **2004**, *306*, 1362–1364.
- (31) Qian, W. Z.; Tian, T.; Guo, C. Y.; Wen, Q.; Li, K. J.; Zhang, H. B.; Shi, H. B.; Wang, D. Z.; Liu, Y.; Zhang, Q.; Zhang, Y. X.; Wei, F.; Wang, Z. W.; Li, X. D.; Li, Y. D. *J. Phys. Chem. C* **2008**, *112*, 7588–7593.
- (32) Lu, C. G.; Liu, J. *J. Phys. Chem. B* **2006**, *110*, 20254–20257.
- (33) Ghosh, S.; Bachilo, S. M.; Weisman, R. B. *Nat. Nanotechnol.* **2010**, *5*, 443–450.
- (34) Fort, E. H.; Donovan, P. M.; Scott, L. T. *J. Am. Chem. Soc.* **2009**, *131*, 16006–16007.
- (35) Khan, M. S.; Crynes, B. L. *Ind. Eng. Chem.* **1970**, *62*, 54–59.
- (36) Wullenkord, M. *Determination of Kinetic Parameters of the Thermal Dissociation of Methane*, Ph.D. Dissertation; German Aerospace Center, Germany, 2011.
- (37) Abanades, S.; Flamant, G. *Int. J. Hydrogen Energy* **2005**, *30*, 843–853.
- (38) Li, H. B.; Page, A. J.; Irle, S.; Morokuma, K. *ChemPhysChem* **2012**, *13*, 1479–1485.
- (39) Bierman, M. J.; Lau, Y. K. A.; Kvit, A. V.; Schmitt, A. L.; Jin, S. *Science* **2008**, *320*, 1060–1063.
- (40) Nanot, S.; Haroz, E. H.; Kim, J. H.; Hauge, R. H.; Kono, J. *Adv. Mater.* **2012**, *24*, 4977–4994.
- (41) Tu, X. M.; Walker, A. R. H.; Khrapin, C. Y.; Zheng, M. J. *Am. Chem. Soc.* **2011**, *133*, 12998–13001.
- (42) Zhu, Z.; Jiang, H.; Susi, T.; Nasibulin, A. G.; Kauppinen, E. I. *J. Am. Chem. Soc.* **2011**, *133*, 1224–1227.
- (43) Kosynkin, D. V.; Higginbotham, A. L.; Sinitskii, A.; Lomeda, J. R.; Dimiev, A.; Price, B. K.; Tour, J. M. *Nature* **2009**, *458*, 872–877.
- (44) Jiao, L. Y.; Zhang, L.; Wang, X. R.; Diankov, G.; Dai, H. J. *Nature* **2009**, *458*, 877–880.
- (45) Wei, D. C.; Xie, L. F.; Lee, K. K.; Hu, Z. B.; Tan, S. H.; Chen, W.; Sow, C. H.; Chen, K. Q.; Liu, Y. Q.; Wee, T. S. *Nat. Commun.* **2013**, *4*, 1374.